Flight Performance of the Biological Lifting Surface

Vasile PRISACARIU*

*Corresponding author
"Henri Coanda" Air Force Academy,
160 Mihai Viteazul Street, Braşov 5001833, Romania,
aerosavelli73@yahoo.com

DOI: 10.13111/2066-8201.2017.9.3.7

Received: 24 June 2017/ Accepted: 24 July 2017/ Published: September 2017

Abstract: *In the international research, biomimetic lifting surface are analyzed in various aspects: construction, aerodynamics and energy. The specificity of the flying wings determined similarity between the aeromechanical and the biomimetic concepts leading to numerous challenges in terms of construction, aerodynamics and actuation. The Aeromechanics of the biological flight focuses both on the various forms of lifting surfaces and the biomechanical aspects. This article contains a number of references to the biological inspiration of the morphing concept, a brief introduction to the theoretical area of the flying wings and a numerical analysis of biologically similar morphing geometry completed by conclusions and future approaches.*

Key Words: *wing birds, morphing wing, VLM analysis, flying wing, XFLR5*

ABBREVIATIONS AND SYMBOLS

G	*- weight (N)*	λ	*- aspect ratio (-)*	V_z	*- vertical speed (m/s)*
S	*- surface (m^2)*	α	*- incidence (^{0}), AoA*	V, V_{xy}	*- horizontal speed (m/s)*
L	*- lift*	*AoA*	*- angle of attack*	C_L	*- lift coef.*
C_m	*- pitch moment coef.*	C_n	*- yaw moment coef.*	C_l	*- roll moment coef.*
υ	*- kinematics viscosity*	*BM*	*- bending moment*	C_D	*- drag coefficient*
MAC	*- mean aerodynamic chord*	*ISTAR*	*- intelligence, surveillance, target acquisition, and reconnaissance*		
VLM	*- vortex lattice method*				

1. INTRODUCTION

1.1 Biological inspiration of flight. Flight types

Flight is the main mode of locomotion used by most species of birds for feeding, breeding and avoiding the predators. Researchers have been inspired by the basics of biological flight in order to develop aerial machines in the concept of morphing.

Aeromechanical biological flight is based on three fundamental movements of the wings: the swing movement, the twisting and the tilting movement, see Figure 1. In order to control the flight according to morphing concept for the soaring and maneuvering flights our approach only choose the wings movements of torsion and tilting along the span, transposed to the mini UAV lifting surfaces.

Specialized references [1, 3, 22, 23] provide a number of instances of birds in flight float and maneuver sequences, see Figure 2.

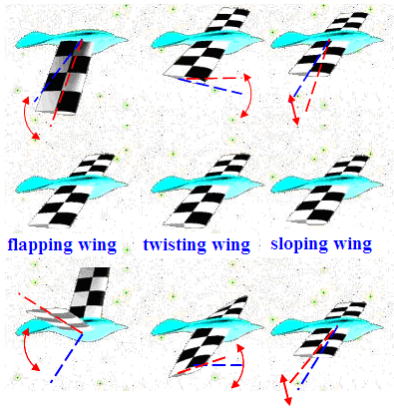

Fig. 1 Fundamental movements of the biological flight

Fig. 2 Bald Eagle [1]

According to [2, 4] we have the angles (α), the force of lift (*L*) and speeds in soaring flight see Figures 3 and 4.

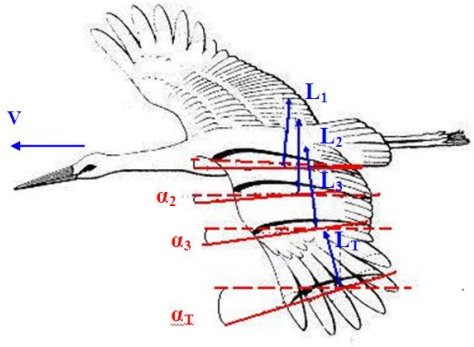

Fig. 3 Angles and lifting on the biological wing [2, 4]

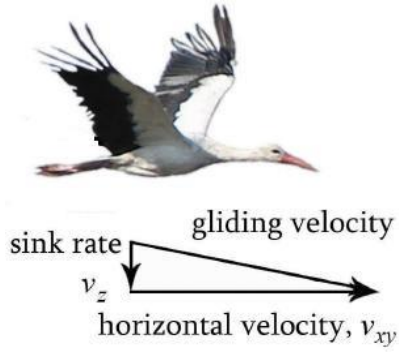

Fig. 4 Speeds for the soaring flight [2, 4]

Wing planform and classes of flight

The shape of the wing is an important factor in determining the flight type, so that different forms lead to various compromises between the characteristics and performances such as speed, power consumption, maneuverability. Wing is characterized by two important factors: the aspect ratio (λ) and wing loading (G/S).

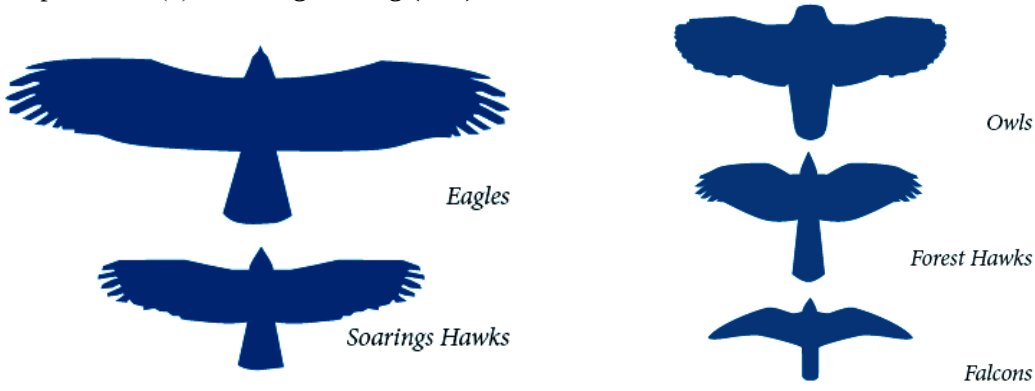

Fig. 5 Types of the biological wings [5]

Biological lifting surfaces can be classified into four main groups as follows: elliptical wings (short and rounded) with small elongation (hawks, sparrows, partridges), high-speed wings (peregrine falcons, ducks), high elongation wings (kestrels, sea birds - cormorants, herons) and soaring flight and high elongation wings (eagles, pelicans, storks), see Figure 5 [5]. The literature [2, 6, 14, 17] provides data for flight characteristics of the bird species that use soaring flight, see Table 1. The frigate has the lowest wing loading (36.5 N/m^2) having therefore the smallest turning radius; however, it can not take off from horizontal surfaces unlike the pelican, and the vulture is best to land and take off in crowded and bumpy areas.

Table 1. Flight features [2, 6, 14, 17]

Birds / **Features**			
	Frigate bird	**Brown pelican**	**Black vulture**
Wing span (m)	2.29	2.10	1.38
Aspect ratio	12.8	9.8	5.8
Wing loading (N/m^2)	36.5	57.8	54.7
C_L	1.33	1.45	1.35
Circling radius (m)	12	18	17

1.2 The current state of the UAV type flying wings

According to [7, 10, 11] for a comparative approached we present the UAV categories that include a series of flying wings with geometries comparable to those from the biological environment, see Figure 6 and Table 2.

Orbiter, USA (miniUAV) [7]

Fulmar, Spania [10]

Eagle Scan, SUA [11]

Fig. 6 Flying wings

Table 2. Features and performances for the flying wings [7, 9, 10]

Orbiter I	Span	2.2 m	Max T/O Weight	7 kg
	Speed	55-130 km/h	Service ceiling	5400 m
	Range	15-30 km	Missions	ISTAR, artillery mode
Fulmar	Span	3 m	Max T/O Weight	20 kg
	Speed	100 km/h	Service ceiling	4000 m
	Range	800 km	Missions	ISTAR
Eagle Scan	Span	3.11 m	Max T/O Weight	22 kg
	Speed	110 km/h	Service ceiling	5950 m
	Range	1500 km	Missions	ISR

2. THEORETICAL REFERENCES

For a 2D vision, professional references [12, 13, 21] indicates a series of biological aerodynamic profiles of the flying wings (Figure 7) and airfoil variation of the biological wing [18, 19], see Figure 8.

From figure 7 common features of biological airfoils of the wings can be noticed: both the large curvature on the upper side of the profile and the thinned trailing edge of the wing airfoil and the spanwise variation with the change in the local angle of incidence (Figure 8).

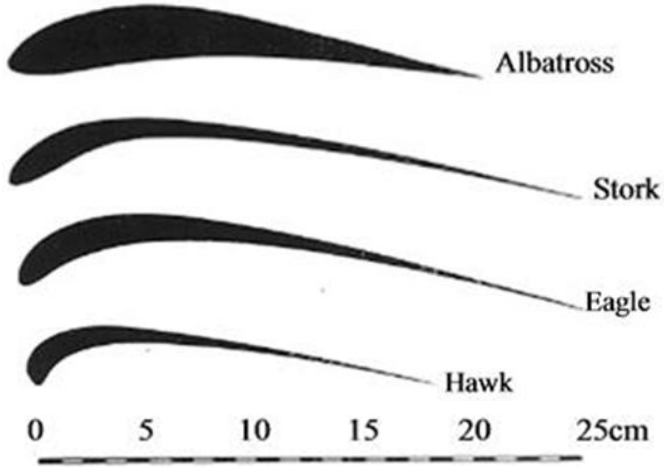

Fig. 7 Airfoils – biological lifting surface (biological wings) [12], [13], [17], [21]

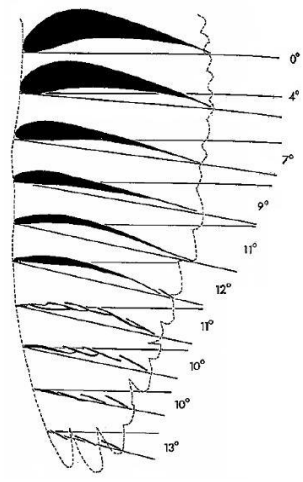

Fig. 8 Stork wing [18], [19]

According to the references and research in the field [14, 15, 20] we can identify aerodynamic airfoils similar to the biological ones, see Figure 9.

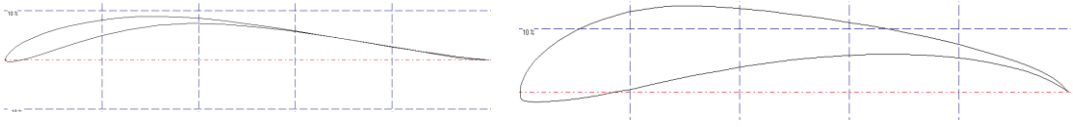

a. Eppler 378 b. S 1223

Fig. 9 Biologically equivalent airfoils [14], [15], [20]

3. AERODYNAMIC ANALYSIS

3.1 2D analysis

For a 2D analysis Eppler 378 airfoil family (see Figure 10) and XFLR5 freeware tool v.6.06 (code Xfoil) are utilized [16]. The analysis conditions are shown in Table 3. The airfoils provide a series of polars numerically analyzed and highlighted in Table 4 and graphically shown in Figure 11 (a, b, c, d).

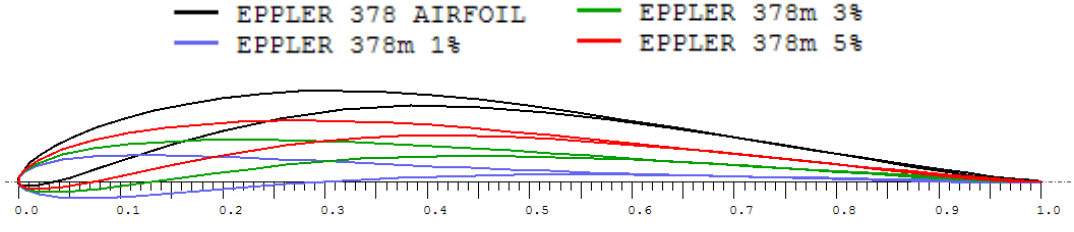

Fig. 10 Eppler 378 family airfoils [16]

Table 3. 2D analysis conditions [16]

Speed (V)	10 m/s	Reynolds number (Re)	342000
Chord	0,5 m	Cinematic viscosity (υ)	1,5 x 10^{+5}
Density (ρ)	1,22 kg/m^3	AoA range analysis (α)	-5÷15^0

Table 4. Numerical data, Eppler 378 airfoil [16]

Calculated polar for: EPPLER 378 AIRFOIL

1 1 Reynolds number fixed Mach number fixed

xtrf = 1.000 (top) 1.000 (bottom)
Mach = 0.030 Re = 0.342 e 6 Ncrit = 9.000

alpha	CL	CD	CDp	Cm	Top Xtr	Bot Xtr	Cpmin	Chinge	XCp
-4.000	-0.0470	0.06666	0.06288	-0.0230	0.6083	0.0120	-0.8927	0.0000	-0.2512
-3.000	0.0833	0.05525	0.05134	-0.0443	0.5922	0.0166	-0.9271	0.0000	0.7898
-2.000	0.2067	0.04485	0.04084	-0.0577	0.5767	0.0248	-0.6303	0.0000	0.5325
-1.000	0.3760	0.03586	0.03137	-0.0768	0.5578	0.0293	-0.7000	0.0000	0.4554
0.000	0.5430	0.02217	0.01702	-0.0920	0.5415	0.0228	-0.8048	0.0000	0.4190
1.000	0.6829	0.01309	0.00653	-0.0969	0.5221	0.0364	-0.9027	0.0000	0.3899
2.000	0.7945	0.01235	0.00528	-0.0960	0.4973	0.0866	-0.9987	0.0000	0.3678
3.000	0.9044	0.01173	0.00463	-0.0951	0.4856	0.1207	-1.1113	0.0000	0.3511
4.000	1.0123	0.01157	0.00456	-0.0940	0.4661	0.1710	-1.2590	0.0000	0.3376
5.000	1.1190	0.01204	0.00520	-0.0932	0.4445	0.2536	-1.4722	0.0000	0.3268
6.000	1.2347	0.01136	0.00533	-0.0943	0.4180	1.0000	-1.8063	0.0000	0.3185
7.000	1.3390	0.01196	0.00605	-0.0932	0.3872	1.0000	-2.2769	0.0000	0.3103
8.000	1.4221	0.01596	0.00876	-0.0918	0.1231	1.0000	-3.3736	0.0000	0.3035
9.000	1.4891	0.02217	0.01428	-0.0893	0.0039	1.0000	-4.5465	0.0000	0.2974
10.000	1.5460	0.02763	0.02054	-0.0861	0.0032	1.0000	-5.6531	0.0000	0.2913
11.000	1.5295	0.04051	0.03425	-0.0872	0.0031	1.0000	-6.1105	0.0000	0.2907
12.000	1.4993	0.05558	0.04991	-0.0873	0.0032	1.0000	-6.3963	0.0000	0.2900
13.000	1.4700	0.07117	0.06609	-0.0872	0.0034	1.0000	-6.6099	0.0000	0.2892
14.000	1.4397	0.08973	0.08538	-0.0894	0.0037	1.0000	-6.6579	0.0000	0.2901
15.000	1.3897	0.11387	0.11032	-0.0988	0.0040	1.0000	-6.3664	0.0000	0.2973

Eppler 378 airfoil (unchanged) generates a maximum lift coefficient C_L= 1.45 to 10^0 AoA (Figure 11 a) and a drag coefficient C_D = 0.018 in the AoA = 3^0 ... 7^0 (Figure 11 d). The maximum glide ratio (C_L/C_D) has a value of 7^0 AoA and the minimum coefficient pitch moment C_m is performed in the AoA range = $2^0 \div 6^0$.

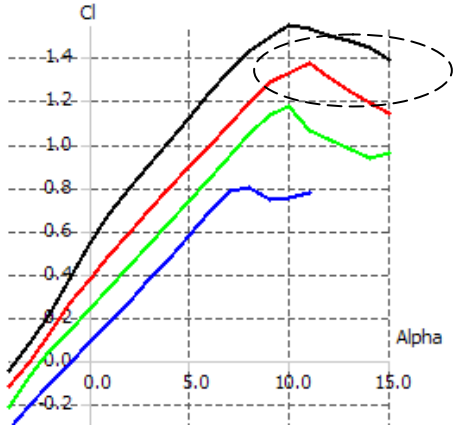

a. C_L-AoA

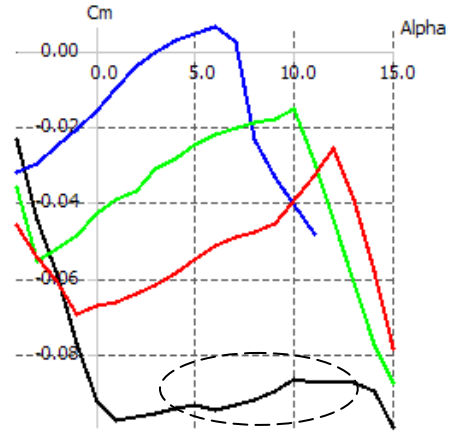

b. C_m-AoA

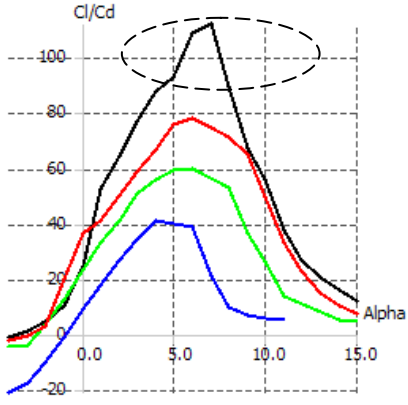

c. C_L/C_D-AoA

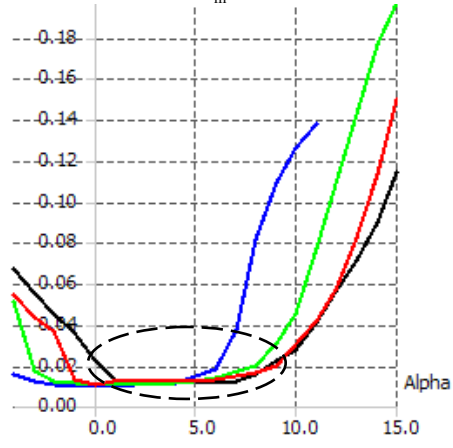

d. C_D-AoA

Fig. 11 Polars Eppler 378 airfoil [16]

3.2 3D Analysis

We propose to analyze a lifting surface of flying wing type (gull wing) in concept morphing having a geometry similar to that of the bald eagle, see Table 5 and Figure 12; the analysis is performed by the freeware tool XFLR5 6.06 [16].

Table 5. Features of bald eagle [17]

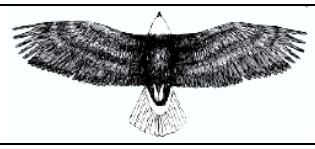	Data	Value	Data	Value
	Span (m)	1.8 – 2.4	Length (m)	0.7 – 0.96
	Mass (kg)	2.6 -5.2	Flight type	Slow flapping, soaring

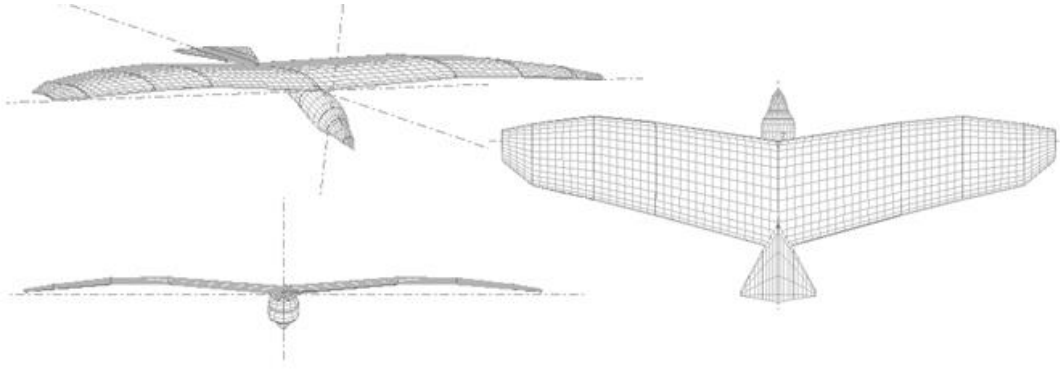

Fig. 12 Flying wing analysis [17]

The analysis was performed on a 3D configuration in gliding flight (see Figure 11) having the characteristics and initial conditions shown in Table 6.

The graphs in Fig. 13 present a lifting surface in two comparative configurations with wingtips Eppler 378 and Eppler 378 1%, with highlighting of the aerodynamic coefficients and moment coefficients.

Table 6. Features and analysis conditions

Features			
Characteristics	*Value*	*Characteristics*	*Value*
Span	1.8 m	Aspect ratio	6.51
MAC	0.29 m	Surface	0.5 m^2
Weight	2.7 kg	Wing loading	5.4 kg/m^2
Analysis conditions			
Characteristics	*Value*	*Characteristics*	*Value*
Speed analysis	10 m/s	VLM panels wing	10150
Method analysis	3D panes/VLM inviscid	3D panels wing	2100
AoA range analysis	$-4^0 \ldots 16^0$	Max. iteration	200
Tip / Root Reynolds	66000 / 233000	Boundary conditions 3D	Neumann

The analysis characteristics are selected in view to have the similar flight conditions of the biological wings.

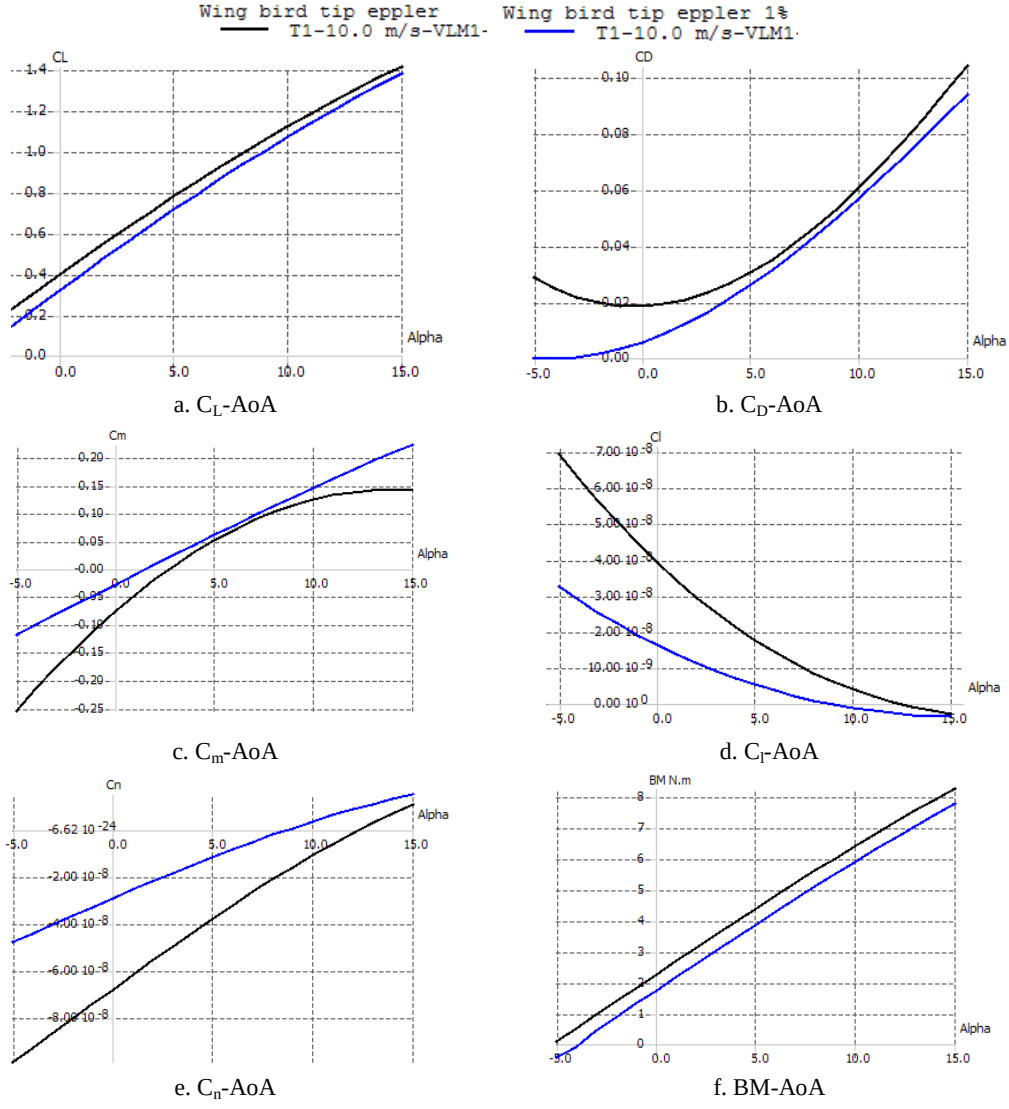

a. C_L-AoA b. C_D-AoA

c. C_m-AoA d. C_l-AoA

e. C_n-AoA f. BM-AoA

Fig. 13 Flying wing polars (chart)

For the evolution in the gliding/soaring flight for the 4^0-12^0 AoA range, differences of the lift, drag and moment coefficients behavior (leading edge of the wing MAC),which are shown in Fig.13 and listed in Table 7, can be noticed at both configurations.

Table 7 Aerodynamic features –flying wings (Eppler tip/ NACA tip) for AoA 5^0

Characteristics	Eppler 378 / Eppler 378 1%	Characteristics	Eppler 378/ Eppler 378 1%
C_L	0.77 / 0.71	C_m	0.052 / 0.061
C_D	0.030 / 0.025	C_L/C_D	25.57 /27.44
C_l	17.7 x 10^{-9} / 5.32 x 10^{-9}	BM (Nm)	4.37 / 3.86

In Figure 13c a longitudinal instability of both configurations with neutral steering, highlighted by reverse slope of the pitch coefficient time can be noticed. For the correct slope of the coefficient stability it is necessary the action of the tail assembly to a negative angle of incidence.

Although a decreasing of the lift coefficient (C_L) to the wingtips with Eppler 378 profile (1% curvature) can be noticed a better behavior regarding C_D, glide ratio (C_L/C_D) and the bending moment coefficient (BM) can be observed because of the pressure discharges to the extremal areas of the lifting surfaces, see Figure 13 and figures 14-19.

To improve the flow wingtips negative or twisted wing, winglets, [24, 25, 26] or blowing boundary layer with the Coanda effect in these areas [27, 28, 29] should be adopted.

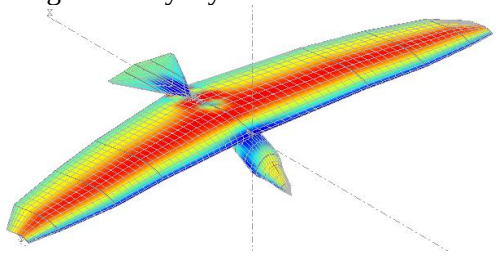

Fig. 14 C_p for AoA = 0^0 wing tip Eppler 378

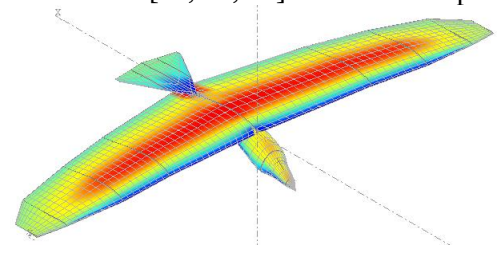

Fig. 15 C_p for AoA = 0^0 wing tip Eppler 378 1%

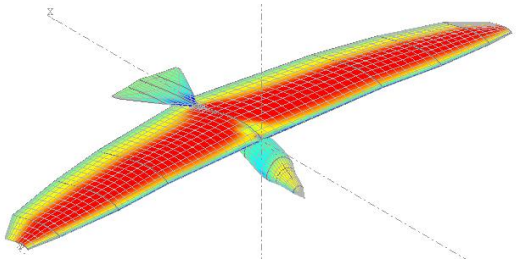

Fig. 16 C_p for AoA = 5^0 wing tip Eppler 378

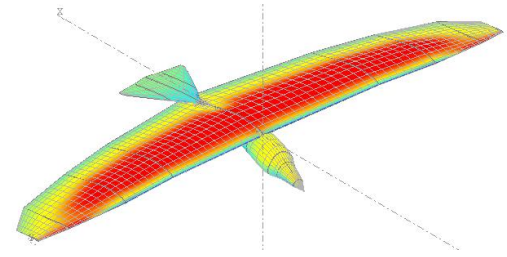

Fig. 17 C_p for AoA = 5^0 wing tip Eppler 378 1%

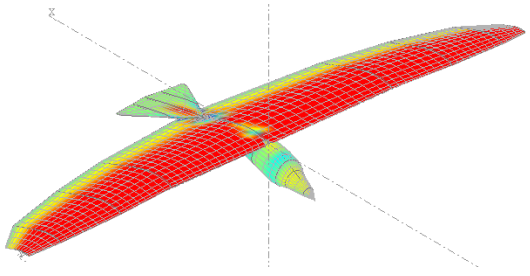

Fig. 18 C_p for AoA = 10^0 wing tip Eppler 378

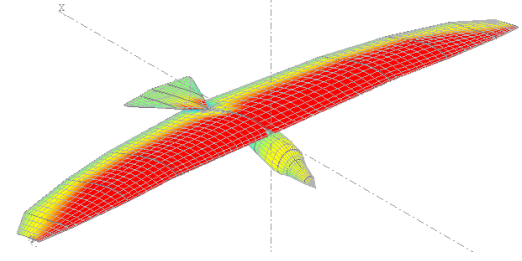

Fig. 19 C_p for AoA = 10^0 wing tip Eppler 378 1%

As expected, a more intense flow for curved wingtips (Eppler 378) versus planar wing tips (378 Eppler same profile curvature 1%) can be noticed in Figure 20.

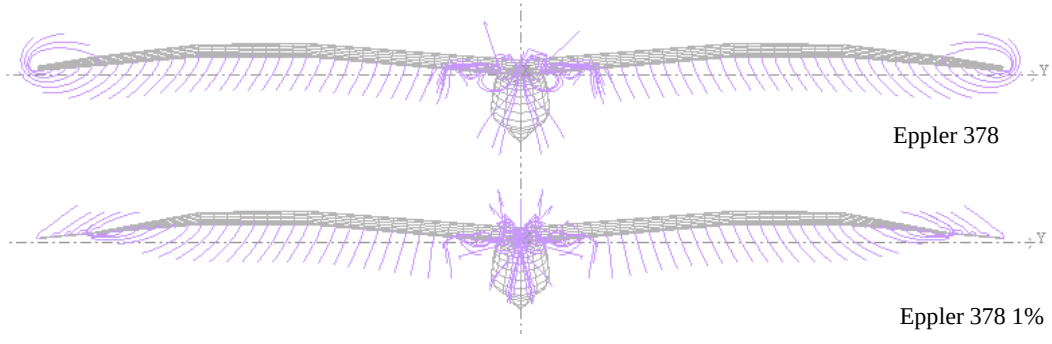

Fig. 20 Air flow for tip wings (AoA=0^0)

Induced drag is highlighted in Figure 21 with a significant decrease in extreme areas of the wings (trailing edge).

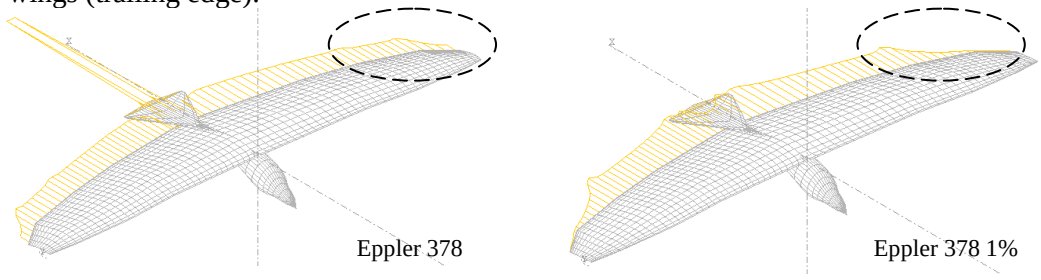

Fig. 21 Induced drag

4. CONCLUSIONS

The software tools used in this analysis determine a trusted range of results that sometimes requires a high degree of refinement proportional to the design approach error value and the methods used.

This article reveals aspects of aeromechanical aspects of the flying wing lifting surfaces, analyzed based on geometry similar to the biological one, focusing only on the characteristics and aerodynamic performance of the lifting surfaces extremities.

Obtaining optimized results involves the use of a 2D geometric similarities package (biological geometric profiles), 3D (in plan form of the bearing surfaces) and mass similarities (total mass and balance) with higher degrees of refinement.

To analyze the maneuver control in gliding/soaring flight (without wings flapping) initial conditions for aerodynamic simulation are required for characteristic angles of the lifting surfaces (eg: the dihedral angle of the wing, lateral and longitudinal angles of the tail assembly/tail). Validation of the results with free software tools should be compared with commercial CFD codes (i.e., Solidworks-Floworks, Ansys-Fluent) which provide a high degree of confidence on the pre-processing and post-processing data analysis, [29, 30].

ACKNOWLEDGMENT

The authors wish to thank to "Henri Coandă" Air Force Academy of Braşov for supporting the research necessary for writing this article.

REFERENCES

[1] C. Phillip, foto, available at http://www.oceanlight.com/lightbox.php, accessed at 12.03.2017.
[2] * * * http://www.wfis.uni.lodz.pl/edu/Proposal.htm, accessed at 14.03.2017.
[3] M. Brooke, T. Birkhead (editori). *Cambridge Enciclopedia de Ornitologie*, Cambridge, Cambridge University Press ISBN 0-521-36205-9, 1991.
[4] Z. Ákos, M. Nagy, S. Leven and T. Vicsek, *Thermal soaring flight of birds and UAVs*, disponible at www.arxiv.org/pdf/1012.0434.
[5] O. Lilienthal, *Birdflight as the basis of aviation, a contribution towards a system of aviation*, Longmans, Green, and Co., 39 Paternoster row, London, New York, Bombay, Calcutta, 172p, 1911.
[6] C. J. Pennycuick, Thermal soaring compared in three dissimilar tropical bird species, Fregata Magnificens, Pelecanus Occidentalis and Coragyps Atratus, *Journal of Experimental Biology*, 102: 307-325, 1983.
[7] * * * UAS Yearbook, *Unmanned aircraft systems – The Global Perspective 2011/2012*, Blyenburg & Co, Paris, ISSN 1967-1709, 216 p, june 2011.
[8] R. Coppinger, *Aurora Flight Sciences' solar powered UAV flies*, 2009, available at

http://www.flightglobal.com/news/articles/aurora-flight-sciences39-solar-powered-uav-flies-326896, accessed at 11.03.2017.
[9] * * * http://www.aeronautics-sys.com/?CategoryID=262&ArticleID=219&SearchParam=orbiter accessed at 11.03.2017.
[10] * * * Thales, *Fulmar features*, Spania, available at https://www.thalesgroup.com/sites/default /files/asset/document/fulmar-ing200214.pdf , accessed at 04.03.2017.
[11] * * * Insitu, Scan Eagle Backgrounder, PR073113, 10p, available at http://www.boeing.com/ farnborough2014/pdf/BDS/ScanEagle%20Backgrounder%200114.pdf.
[12] G. Pfeifhofer, H. Tributsch, *The Flight of Albatross—How to Transform It into Aerodynamic Engineering?*, Engineering, 2014, 6, p.427-438, Published Online July 2014 in SciRes. http://www.scirp.org/journal/eng, http://dx.doi.org /10.4236/eng.2014.68045.
[13] B. R. Munson, T. H. Okiishi, D. F. Young, *Fundamentals of Fluid Mechanics*. 4th Edition, R. R. Donnelley & Sons, Chicago, 2002.
[14] V. A. Tucker, Gliding birds: the effect of variable wing span, *Journal* of *Experimental Biology*, vol. **133**, 33-58, 1987.
[15] * * * http://www2.unil.ch/biomapper/opengl/BirdFlight.html.
[16] M. Drela, H. Yungren, *Guidelines for XFLR5 v6.03 (Analysis of foils and wings operating at low Reynolds numbers)*, 2011, available at http://sourceforge.net/projects/xflr5/files; accessed at 12.03.2017.
[17] * * * *Bald eagle (Haliaeetus leucocephalus)*, available at http://www.wildlife.state.nh.us /Wildlife/ Wildlife_profiles/bald_eagle.html, accessed at 19.03.2017.
[18] T. Chklovski, *Pointed-Tip Wings at Low Reynolds Numbers*, available at http://www.wfis.uni.lodz.pl/edu/Proposal.htm, accessed at 07.03.2017.
[19] H. V. W. Nachtigall and J. Wieser, Profilmessungen am Taubenflugel, *Zeit. Vergl. Physiol*. **52**: 333-346, 1966.
[20] T. Liu, Avian Wing Geometry and Kinematics, *AIAA JOURNAL*, Vol. **44**, No. 5, ISSN: 0001-1452, p 954-963, May 2006.
[21] V. A. Tucker, G. C. Parrot, Aerodynamics of gliding flight in a falcon and others birds, *Journal Exp. Biol.*, **52**, p. 345-367, 1970.
[22] * * * http://www.bou.org.uk/birds-and-dynamic-soaring , accessed at 27.09.2016.
[23] M. B. E. Boslough, *Autonomous Dynamic Soaring Platform for Distributed Mobile Sensor Arrays*, SAND REPORT, SAND 2002-1896, Sandia Corporation-Lockheed Martin Company, USA, 54p, 2002.
[24] V. Prisacariu, I. Cîrciu, M. Boşcoianu, Morphing concept of UAVs of the swept flying wing, *RECENT journal*, ISSN 1582-0246, vol. **15**, 1(41), p26-33, 2014.
[25] S. Rajendran, *Design of Parametric Winglets and Wing tip devices – A Conceptual Design Approach*, Linkoping University, SE-58183 Linköping, Sweden, 71p, 2012.
[26] R. K. Nangia, M. E. Palmer, R. H. Doe, *Aerodynamic Design Studies of Conventional & Unconventional Wings with Winglets*, 24th Applied Aerodynamics Conference 5 - 8 June 2006, San Francisco, California, AIAA 2006-3460, 18p.
[27] I. Cîrciu, S. Dinea, Review of applications on Coandă effect history, theories, new trends, *Review of the Air Force Academy*, 2/2010, p 14-21.
[28] H. Coandă, *US Patent no. 3.261.162 "Lifting Device Coanda Effect",* 1936, USA.
[29] I. Cîrciu, D. Luculescu, V. Prisacariu, E. Mihai, C. Rotaru, Theoretical Analysis and Experimental Researches regarding the Asymmetrical Fluid Flow Applied in Aeronautics, *Advances in Materials Science and Engineering*, Hindawi Publishing Corporation, Article ID 681284, 2015, available at https://www.hindawi.com/journals/amse/2015/681284.
[30] V. Prisacariu, C. Boşcoianu, I. Cîrciu, M. Boşcoianu, The Limits of Downsizing –a Critical Analysis of the Limits of the Agile Flying Wing MiniUAV, *Applied Mechanics and Materials*, Vol. **772**, pp 424-429, © (2015) Trans Tech Publications, Switzerland, doi:10.4028/www.scientific.net /AMM.772.424, p. 424-429, 2015.